



Collagen/silicocarnotite composites, cross-linked with chondroitin sulphate: in vitro bioactivity

Lachezar Radev^{1,*}, Vladimir Hristov¹, Irena Michailova¹, Maria H. V. Fernandes², Isabel M. M. Salvado²

¹University of Chemical Technology and Metallurgy, Sofia, Bulgaria

²University of Aveiro and CICECO, Aveiro, Portugal

Received 6 June 2011; received in revised form 12 September 2011; accepted 18 September 2011

Abstract

In this work we present the experimental results on synthesis, structure evolution and in vitro bioactivity of collagen-silicocarnotite-chondroitin sulphate composites. The obtained samples were synthesised by mixing collagen (C) and silicocarnotite (S) powder with C:S ratio of 75:25 and 25:75 wt.% in the presence of chondroitin sulphate (ChS). Collagen was diluted in 5M CH₃COOH before mixing. The obtained materials were characterized by X-ray diffraction (XRD), Fourier-transform infrared (FTIR) spectroscopy and scanning electron microscopy (SEM) before and after in vitro test in 1.5 simulated body fluid. XRD of synthesized samples showed that before immersion carbonate containing hydroxyapatite (CO₃HA) were formed in situ in the composites. FTIR depicts the presence of HPO₄²⁻ and the “red shift” of COO⁻ and SO₃⁻ from ChS was also observed. This “red shift” could be attributed that the ChS prefers to chelate Ca²⁺ from partially dissolved S powder. SEM of the prepared samples show the presence of nanosized hydroxyapatite (HA) whiskers and flower-like HA assemblies. After in vitro test, XRD proved the presence of HA with well-defined crystallinity. According to the FTIR results B-type CO₃HA can be observed. SEM of the precipitated layers show the presence of HA spheres. Inductively coupled plasma atomic emission spectroscopy results lead to a conclusion that after in vitro test of the prepared composites silicon containing carbonate substituted hydroxyapatite (Si-CO₃HA) may be formed on the surface of the immersed samples.

Keywords: silicocarnotite, collagen, chondroitin sulphate, hydroxyapatite whiskers, in vitro bioactivity

1. Introduction

Bones and teeth consist of biocomposites with well-organized nanostructured hydroxyapatite (HA) to perform important biological functions. It is well documented that the ordered structures in mineralized tissues appeared to originate from organized assemblies of biomolecules, such as collagen, polysaccharides and proteoglycans [1–3]. Previous articles indicate that some biomacromolecules are added for controlling the nucleation, growth and size of calcium phosphate phases. Chondroitin-4-sulphate (ChS) is just one of these molecules. It consists of a repeating disaccharide unit of D-glucuronic acid linked to N-acetylgalactosamine. The galactosamine residues are sulphated

in position 4 [4]. It is obvious that galactosamine belongs to the family of glycosaminoglycans, which can be found on cell surfaces and the extracellular matrix of cartilage and bone [4–6]. The aim of some preliminary results is to contribute to the understanding of the role of ChS in biomineralization process [7–15]. Some studies show that ChS is an inhibitor of HA formation and growth from the calcium phosphate solutions, as well as an inhibitor of transformation of so-called amorphous calcium phosphate to crystalline HA [8,14]. Other studies show that the combination of sulphate and carboxylate groups gives a very high density of negative charge and may allow them to act as nucleation sites for the HA formation [11,12,15]. Despite these papers, all authors summarized that the self-assembly of the HA crystals is critically dependent on

* Corresponding author: tel: +35 92 816 3280
fax: +35 92 868 5488, e-mail: l_radev@abv.bg

the chemical interactions between the HA crystals and the functional groups of ChS. The nucleation models are based on the binding of Ca^{2+} to the periodically arrayed functional groups of ChS [7–15].

In our previous work we have synthesized some bioactive calcium phosphate silicate (CPS) ceramics [16]. The obtained ceramic powders were in vitro bioactive in 1.5SBF for different periods of time. On the bases of the prepared ceramics, we have produced in vitro bioactive composites with gelatin and collagen [17,18] without cross-linkage.

The purpose of this article is to prepare and characterize collagen/silicocarnotite composites, obtained from collagen (C) and silicocarnotite (S) in the presence of ChS and investigate their in vitro bioactivity.

II. Experimental

2.1 Preparation of the composites

The silicocarnotite powder, the inorganic part of the composites, has been synthesized via multi-step sol-gel method. The molar ratio Ca/P+Si of the chemical composition from initially prepared silicocarnotite sol, as described as 58.12 wt.% CaO, 29.4 wt.% P_2O_5 , 12.45 SiO_2 wt.%, was equal to 1.67. The procedure for the synthesis and structure evolution of the obtained ceramic powder was described in our previous work [16]. Collagen type I, taken in amounts corresponding to the composite content, was diluted in 20 ml 5M CH_3COOH for 24 h at room temperature. The C-S composite materials, for two types of proportions 25:75 and 75:25 wt.% were prepared by adding S to the C solution with constant intensive stirring for 6 h. pH of the obtained mixture was 2. After homogenation time, pH was adjusted to 9 using 25% NH_4OH . ChS was added as cross-linking agent. The obtained composite materials were dried at 70°C for 12 h under vacuum.

2.2 In vitro test for bioactivity

Bioactivity of obtained composites was evaluated by examining the apatite formation on their surfaces in 1.5SBF solution. The 1.5SBF solution was prepared from reagents as follows: $\text{NaCl} = 11.9925$ g, $\text{NaHCO}_3 = 0.5295$ g, $\text{KCl} = 0.3360$ g, $\text{K}_2\text{HPO}_4 \times 3\text{H}_2\text{O} = 0.3420$ g, $\text{MgCl}_2 \times 6\text{H}_2\text{O} = 0.4575$ g, $\text{CaCl}_2 \times 2\text{H}_2\text{O} = 0.5520$ g, $\text{Na}_2\text{SO}_4 = 0.1065$ g, and buffering at pH 7.4 at 36.5°C with 9.0075 g of *tris*(hydroxymethyl)aminomethane (TRIS) and 1M HCl in distilled water. The synthesised composites were pressed at 50 MPa with PVA to obtain disc specimens (12 mm diameter and 2 mm thick) and immersed in 1.5SBF at the human body temperature (36.6°C) in polyethylene bottles in static conditions for 3 days. A few drops of 0.5% sodium amide (NaN_3) were added to the 1.5SBF solution to inhibit the growth of bacteria [19]. After soaking, the specimens were removed from the fluid, gently rinsed with distilled water, and then dried at 36.6°C for 12 h.

2.3. Methods for analysis

The structure and in vitro bioactivity of composite materials were monitored by X-ray diffraction (XRD) analysis, Fourier-transform infrared (FTIR) spectroscopy and scanning electron microscopy (SEM). Powder X-ray diffraction spectra were collected within the range from 10° to 80° 2θ with a constant step 0.04° 2θ and counting time 1 s/step on a Bruker D8 Advance diffractometer with $\text{CuK}\alpha$ radiation and SolX detector. The spectra were evaluated with the *DiffraplusEVA* package. FTIR transmission spectra for the obtained samples were recorded by using a Bruker Tensor 27 spectrometer with scanner velocity 10 kHz. KBr pellets were prepared by mixing ~1 mg of the samples with 300 mg KBr. Transmission spectra were recorded using MCT detector, with 64 scans and 1 cm^{-1} resolution. SEM (JEOL, JSM-35 CF, Japan) was used to ascertain the morphology and chemical constituents of the prepared composites before and after immersion in 1.5SBF for 3 days at accelerating voltage of 15 kV. After 3 days of soaking, the samples were taken out from 1.5SBF and the ion concentrations of Ca, P and Si in the solutions were measured by inductively coupled plasma atomic emission spectroscopy (ICP-AES, IRIS 1000, Thermo Elemental, USA).

III. Results and discussion

3.1 Characterization of the obtained composites before in vitro test

Figure 1 presents X-ray diffraction data of the prepared composites with different component weight ratios. From the depicted XRD data, we can observe the presence of carbonate hydroxyapatite (CO_3HA) - PDF 21-0145 and $\text{Ca}_5(\text{PO}_4)_2\text{SiO}_4$ (silicocarnotite) - PDF 40-0309. In addition, an unexpected result is the presence of a large crystalline peak, positioned at 32.59 (2θ). The presence of this peak could be ascribed to the CO_3HA and the crystalline C-S-P-H ($\text{CaO-SiO}_2\text{-P}_2\text{O}_5\text{-H}_2\text{O}$) phase. In accordance with Lee and Kim [20], the presence of crystalline $\text{CaO-SiO}_2\text{-P}_2\text{O}_5\text{-H}_2\text{O}$ phase is a function of partial substitution of amorphous silica by P_2O_5 on the surface of silicocarnotite after hydration reaction.

FTIR spectra of the synthesized C-S composites are shown in Fig. 2. As can be seen, the obtained FTIR spectra have very complicated character. The bands centred at 955 cm^{-1} were assigned to the Si-O-Si asymmetric stretch vibrations [21–23] and the bands at 562 cm^{-1} and 467 (473) cm^{-1} to the Si-O-Si bending vibrations [21,23]. The bands posited at 562, 606, 618, 663 and 675 cm^{-1} can be assigned to the presence of $\nu_3\text{SiO}_4^{4-}$ and $\nu_4\text{PO}_4^{3-}$ groups [22,24–27]. The band with small intensity at around 628 cm^{-1} corresponds to the presence of OH^- in silicocarnotite. Radev *et al.* [16] observed that the presence of this band is consistent with the silicon substitution mechanism, proposed as $\text{SiO}_4^{4-} \rightarrow \text{PO}_4^{3-}$. This replacement leads

to decreasing of quantity of some OH⁻ groups, i.e. silicocarnotite is partially dehydroxylated calcium phosphate silicate [16].

The very important vibrations of the PO₄³⁻ in the FTIR spectra, depicted in Fig. 2, could be distinguished in the three main regions: (i) the peak with small intensity posited at 1059 cm⁻¹ (curve a) is associated with asymmetric stretch vibrations [28]; (ii) a weak band at 954 (962) cm⁻¹ for two samples corresponding to the symmetric stretching [27–30] and (iii) two well resolved peaks at 562 cm⁻¹ assigned to the asymmetric modes [30,31]. Furthermore, the presence of a ν₂CO₃²⁻ mode, posited at 857 (860) cm⁻¹ and 892 cm⁻¹ indicates that the synthesised composites were similar to natural bone [32]. Moreover, in accordance with Garnjanagoonchorn *et al.* [6], the peak at approximately 857 (860) cm⁻¹ was used to identify ChS in different sources of cartilage. In our samples the presence of this band verified the experimental procedure.

On the other hand, Tanaka *et al.* [33], assumed that the peak at ~962 cm⁻¹ and these between 1020–1100 cm⁻¹ could be ascribed to the presence of HPO₄²⁻ in the apatite structure. In the FTIR spectrum of the sample with 75 wt.% C and 25 wt.% S, HPO₄²⁻ bands were posited at 960, 1080 and 1208 cm⁻¹ [34,35]. In this case, when silicocarnotite particles are added into acidic collagen solution, some of the silicocarnotite particles will dissolve in the acidic medium and produce Ca²⁺, PO₄³⁻ and SiO₄⁴⁻ ions. Furthermore, PO₄³⁻ can produce HPO₄²⁻ according to the reaction: H⁺ + PO₄³⁻ → HPO₄²⁻. Because of this the dissolution reaction of silicocarnotite is accelerated by the decreasing of pH value, i.e. the acidic collagen solution was supersaturated with Ca²⁺ and PO₄³⁻ ions during the preparation of the composites, and consequently, the reprecipitation of other calcium phosphates occurs.

From a fundamental point of view, the amide groups of polypeptides and proteins possess a number of characteristic vibration modes of group's frequencies. Es-

pecially, the amide I, II and III are directly related to the polypeptide conformation. The amide I band, with a characteristic frequency in the range from 1500 to 1700 cm⁻¹, is associated with the stretching vibration of the C=O (carbonyl group) along the polypeptide backbone [36]. This group is a sensitive marker of a polypeptide secondary structure. In accordance with our preliminary investigations, the amide I band is posited at 1656 cm⁻¹. The amide II is centred at 1550 cm⁻¹ and amide III bands have been detected at 1240 and 1281 cm⁻¹. Amide B is centred at 3081 cm⁻¹. The two bands at 1400 and 1340 cm⁻¹ can be assigned to the presence of COOH and COO⁻ in the spectrum of pure gelatin and collagen [17,18].

As shown in the Fig. 2, the amide I bands have changed and shifted to lower wavenumbers from 1656 cm⁻¹ for pure collagen [17,18] to 1613 (1612) cm⁻¹ for the synthesised composites. This change could be assigned to the presence and the crucial role of ChS. It can be explained as following. In a series of papers Rhee and Tanaka [7–9] found that the asymmetrical stretching modes of COO⁻ and SO₃⁻ ions in ChS were detected at 1632 and 1234 cm⁻¹. They wrote that after formation of hydroxyapatite crystals via biomimetic route, with the use of ChS as a template, these modes were detected at 1613 and 1228 cm⁻¹, respectively. They also noted that the “red shift” caused a chemical interaction between hydroxyapatite crystals and the functional groups of the ChS template during the precipitation [7–9]. In our case, in accordance with the experimental procedure, we can assume that the observed “red shift” (from 1632 cm⁻¹ to 1613 (1612) cm⁻¹ and from 1234 cm⁻¹ to 1227 (1230) cm⁻¹) may be due to the chemical interaction between Ca²⁺ from partially dissolved silicocarnotite and COO⁻ and/or SO₃⁻ from ChS.

It is possible and another interpretation, concerning the presence of bands at 1613 (1612) cm⁻¹ in the pre-

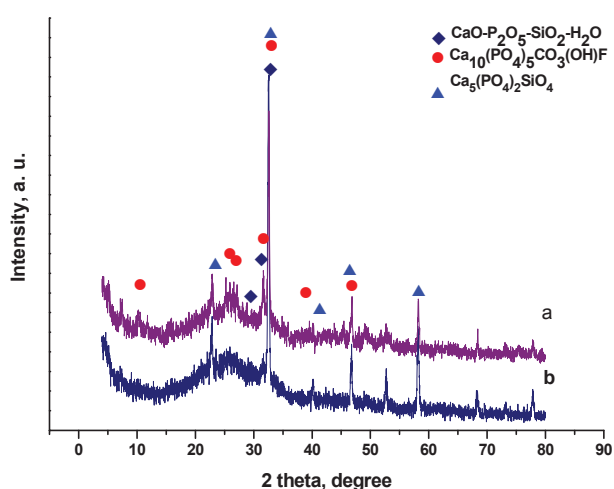


Figure 1. XRD for the prepared C-S samples: 75:25 wt.% (a) and 25:75 wt.% (b)

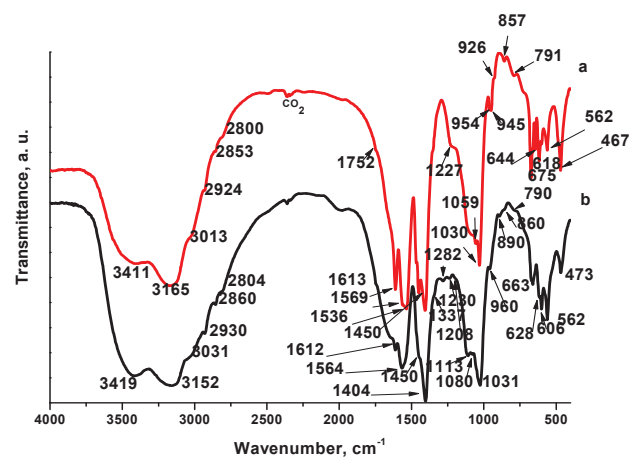


Figure 2. FTIR spectra of C-S samples: 25:75 (a) and 75:25 (b) wt.% before immersion in 1.5SBF

pared composites. Alili [37] shows that amide I bands for denatured and aggregated proteins are posited between 1610 and 1628 cm^{-1} . Liard *et al.* [38] and Petitbois *et al.* [39] found that the band at 1615 cm^{-1} can be assigned to the β -sheet conformation in collagen. Most likely, the presence of the bands at 1613 (1612) cm^{-1} is due to the two processes: (i) chemical interaction between Ca^{2+} and COO^- and/or SO_3^- from ChS and (ii) partial denaturation of collagen in the process of preparation of the composites which leads to the formation of β -sheet structures.

More detailed information about the type of changes of C as an organic part of the synthesized composites was analyzed by the curve fitting in the region 1700–1500 cm^{-1} (Fig. 3). From the presented results, it can be seen that in the 75C:25S wt.% sample (Fig. 3b), new band centred at 1647 cm^{-1} is quite visible. The presence of this band could be ascribed to the chemical interaction between Ca^{2+} from partially dissolved S and C=O amide I from C. In brief, the C=O amide I undergoes “red shift” from 1656 [17,18] to 1647 cm^{-1} for the pre-

pared 75C:25S wt.% sample. From the described data it can be assumed that the collagen goes through two types of changes; (i) “red shift” for C=O amide I and (ii) partial transformation of C molecule to β -sheets conformation under experimental conditions and quantity of C and S of the samples.

The amide II bands in the composites are centred at 1569 (1563) cm^{-1} and at 1535 (1532) cm^{-1} for the composite with weight ratio of the C-S components 25:75 wt.% (Fig. 2, curve a). It was difficult to analyze amide II band in the fields of conformation feature, as it has a complex nature with its vibration source, which arises primarily from the combination of the N-H bending coupled to the C-N stretching vibrations of the peptide linkages [40]. The observed bands can be attributed to the conformation change in collagen, as a result of the chosen method for the preparation of the composites. The amide III does not undergo any changes.

Based on other preliminary results, the absorption bands centred at 1451, 1404, 1337 and 1227 (1230) cm^{-1} may be attributed to the $\delta(\text{CH}_2)$, $\delta(\text{CH}_3)$ and

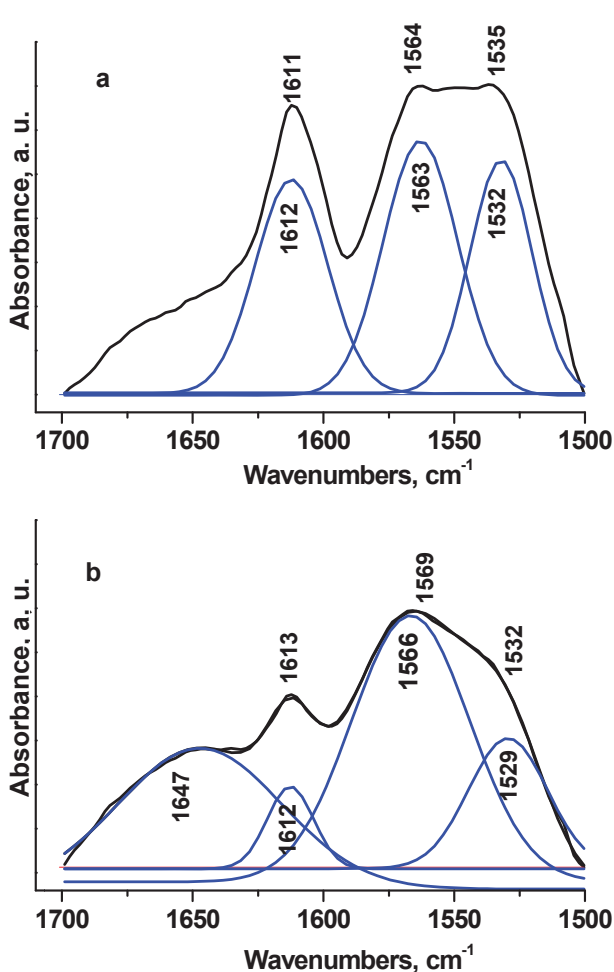


Figure 3. Curve fitting spectra of the C-S samples: 25:75 (a) and 75:25 (b) wt.% before in vitro test in 1.5SBF in the range 1700–1500 cm^{-1}

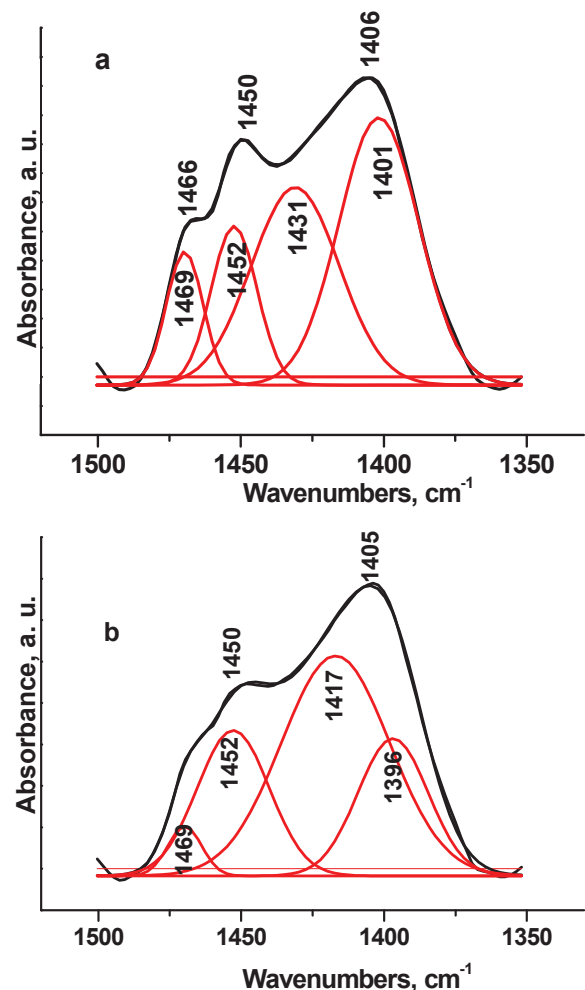


Figure 4. Curve fitting spectra of the C-S samples: 25:75 (a) and 75:25 (b) wt. % before in vitro test in 1.5SBF in the range 1500–1350 cm^{-1}

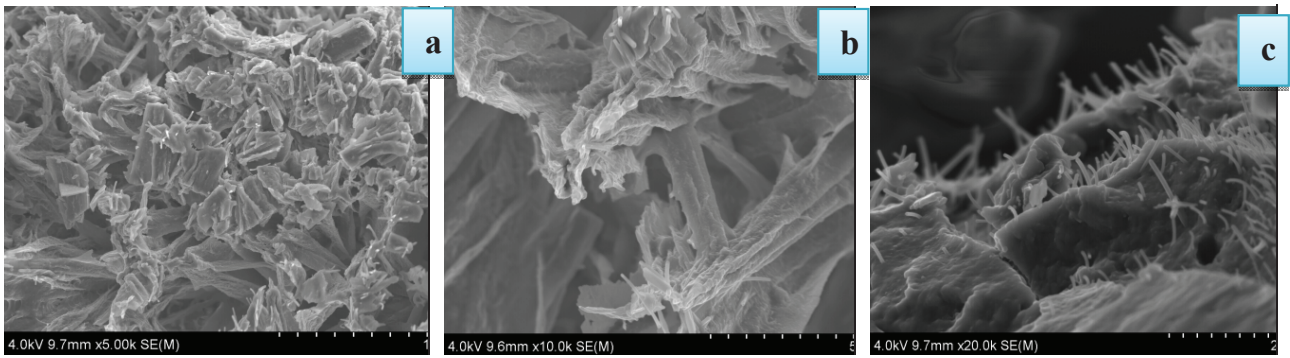


Figure 5. SEM of C-S sample (75:25 wt.%) before SBF at 5000× (a), 10000× (b) and 20000× (c)

v(C-H) absorptions of collagens [39,41]. The band at 1337 cm^{-1} in the C-S composite with 75:25 wt.% (curve b) could be ascribed to the covalent bond formation with Ca^{2+} from partially dissolute silicocarbonite and COO^- from the collagen before soaking in 1.5SBF [7–9]. The band posited at $1227\text{ (}1230\text{)}\text{ cm}^{-1}$ probably corresponds to dehydrate and monohydrate phosphate groups, respectively [42]. In the Fig. 2, the presence of the absorption bands at $1420\text{ (}1418\text{)}\text{ cm}^{-1}$, $1461\text{ (}1457\text{)}\text{ cm}^{-1}$ and 1560 cm^{-1} indicated the formation of carbonate containing calcium phosphates with two types of substitution A-type and B-type before in vitro test [43,44].

Fig. 4 presents more detailed information about curve fitting in the region of $1500\text{--}1350\text{ cm}^{-1}$ of CO_3^{2-} ions in the synthesised C-S samples, before in vitro test in 1.5SBF solution. From the results shown in Fig. 4 results it can be seen that the presence of absorption band at 1417 cm^{-1} (Fig. 4b) indicated the formation of A-type CO_3HA in which $\text{CO}_3^{2-} \rightarrow \text{OH}^-$ [45]. The formation of CO_3HA with B-type substitution in which $\text{CO}_3^{2-} \rightarrow \text{PO}_4^{3-}$ [46,47] is posited firstly at $1401, 1452$ and 1469 cm^{-1} (Fig. 4a) and secondly at $1400, 1452$ and 1469 cm^{-1} (Fig. 4b). Therefore, B- CO_3HA preferentially observed into the C-S samples without reference to the weight ratio of the C and S components of the composites.

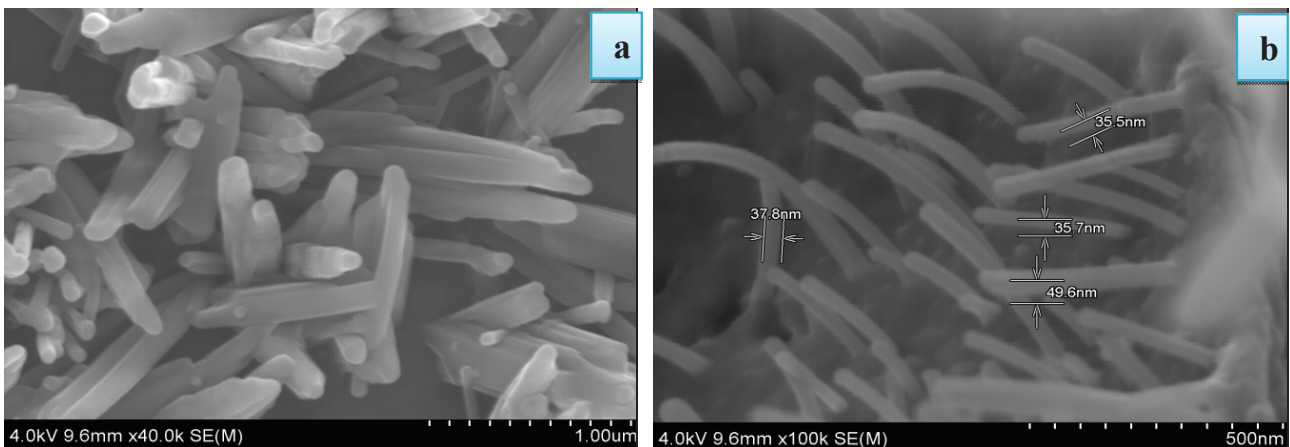


Figure 6. Nano whiskers over C-S sample (75:25 wt.%) at different magnifications: 40000× (a) and 100000× (b) before in vitro test in 1.5SBF

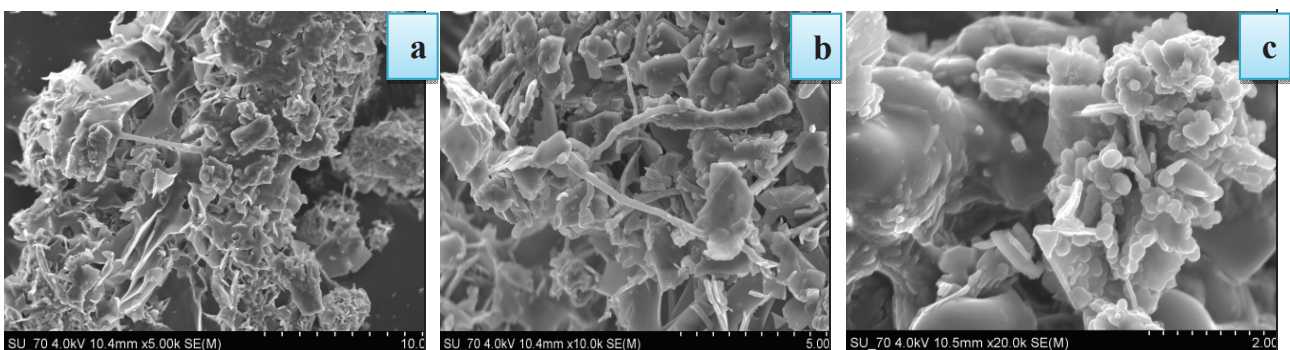


Figure 7. SEM of C-S sample (25:75 wt.%) before SBF at different magnifications: 5000× (a), 10000× (b) and 20000× (c)

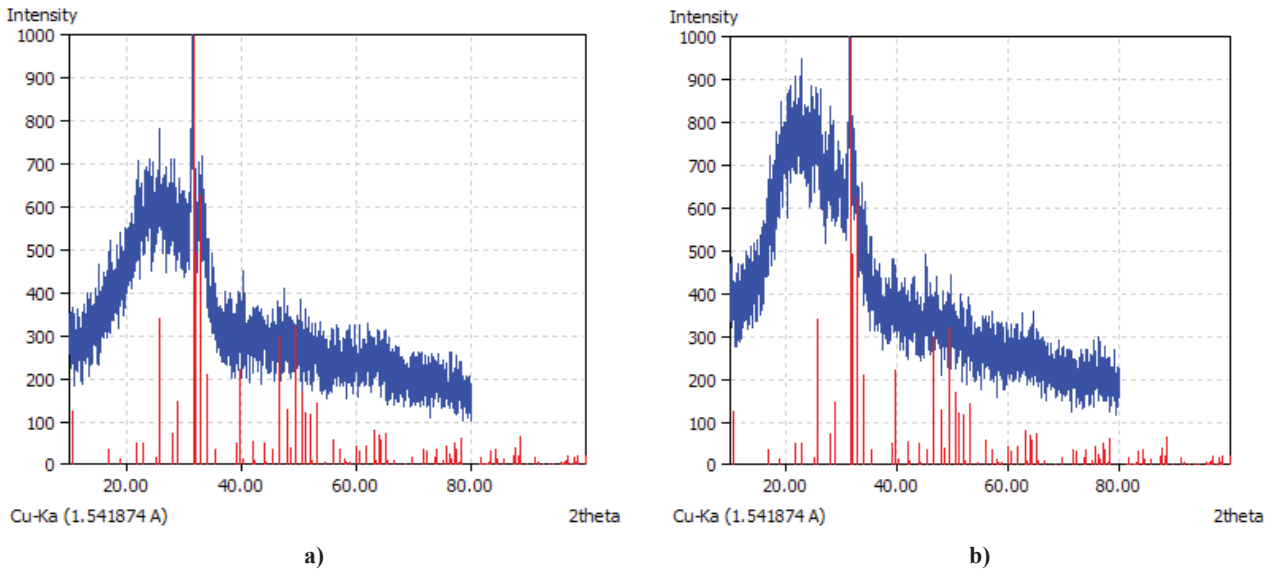


Figure 8. XRD for C-S samples with 25:75 wt.% (a) and 75:25 wt. % (b) after in vitro test

On the FTIR analysis for the prepared composites before in vitro test we can conclude that:

- In the studied samples Ca-deficient HA was formed *in situ* before in vitro test in 1.5SBF: HPO_4^{2-} ions are present in the composite samples.
- Ca^{2+} from the partially dissolved silocarnotite powder may bind with amid I and/or COO^- and form $(\text{C}=\text{O})_2\text{Ca}$ and/or $(\text{COO})_2\text{Ca}$ bonds.
- The collagen undergoes conformation changes due to formation of β -sheet structures.
- The FTIR data confirmed XRD results.

SEM micrographs of the synthesized samples before in vitro test in 1.5SBF are given in Figs. 5 and 6. Figure 5 shows that the C-S composite sample (75:25 wt.%) has a porous microstructure, similar to the bone structure. At high magnification values (Figs. 5c and 6a) the SEM depicts the presence of the monodisperse thin HA whiskers. In coincidence with FTIR data these whiskers consist of Ca-deficient HA. In addition, at very high magnification value (Fig. 5b) it can be seen that Ca-deficient HA is in a nanometer scale.

Figure 7 presents SEM images for C-S (25:75 wt.%) sample before in vitro test. From the SEM images presented in Fig. 7 we can see that the prepared samples have a porous structure and that the Ca-deficient HA has a flower like assembly.

3.2 Characterization of the obtained composites after in vitro test

X-ray diffraction data for the C-S samples after in vitro test in 1.5 SBF in static conditions is given in Fig. 8. From the presented XRD data it can be seen that the well-defined HA (PDF 9-0432) is formed on the composites after immersion in 1.5SBF for 3 days.

The FTIR spectra of prepared C-S composites with weight ratio of the components 75:25 wt.% and 25:75 wt.%, after immersion in 1.5SBF for 3 days are given in Fig. 9.

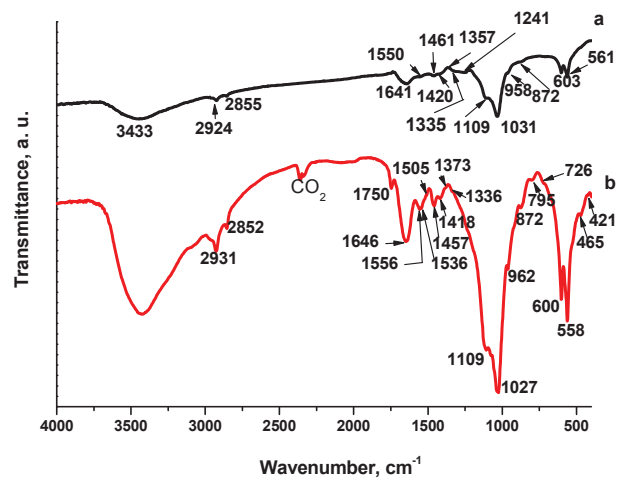


Figure 9. FTIR spectra of C-S composite at 75:25 wt. % (a) and 25:75 wt. % (b) after in vitro test for 3 days in 1.5 SBF

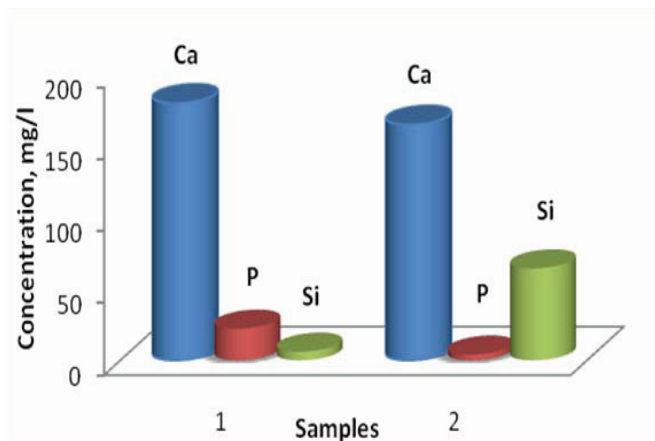


Figure 10. Changes in Ca, P and Si contents from C-S samples: 75:25 wt.% (1) and 25:75 wt.% (2), after soaking in 1.5 SBF for 3 days

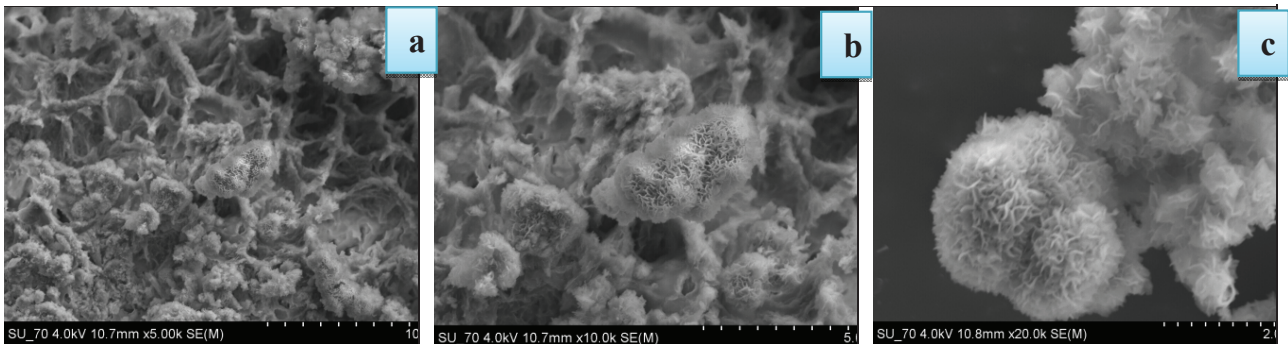


Figure 11. SEM for C-S sample (75:25 wt.%) at different magnifications: 5000× (a) 10000× (b) and 20000× (c)

Figure 9 shows the IR absorption spectra of carbonate containing hydroxyapatite (CO_3HA), formed on the surface of the immersed samples for 3 days in 1.5SBF. The $\nu_1\text{PO}_4^{3-}$ mode is represented in the apatite structure by a band at 958 (962) cm^{-1} , while $\nu_2\text{PO}_4^{3-}$ produces an absorption peak, posited at 465 and 421 cm^{-1} [7–9]. As other authors have noted, the main absorbance signal of PO_4^{3-} appears in the triply degenerate ν_3 domain [48]. The broad peak at around 1029 cm^{-1} (1031 and 1027 cm^{-1} for two samples) is due to both the $\nu_1\text{PO}_4^{3-}$ and $\nu_3\text{PO}_4^{3-}$ and the stronger SiO_4^{4-} band [48]. In addition, the $\nu_2\text{PO}_4^{3-}$ is also masked by the Si-O-Si peak, but the well-defined $\nu_4\text{PO}_4^{3-}$ at 561 (558) cm^{-1} and 603 (600) cm^{-1} are visible [7–9]. Furthermore, among the four internal vibrational modes of CO_3^{2-} , only two are important for the FTIR analysis: ν_2 and ν_3 [49]. The bands posited at 726 and 795 cm^{-1} (Fig. 9, curve b) could be assigned to the presence of small amount of calcite [50,51]. In addition, Feki *et al.* [52] postulated that the bands at ~ 720 cm^{-1} and 872 cm^{-1} could be assigned to the presence of B-type CO_3HA in the immersed samples. The absorption bands at 1357 , 1420 and 1461 cm^{-1} (Fig. 9, curve a) and at 1373 , 1418 , 1457 and 1505 cm^{-1} indicated the formation of CO_3HA with B-substitution in which $\text{CO}_3^{2-} \rightarrow \text{PO}_4^{3-}$ [53].

The 1340 cm^{-1} band in collagen, as has been written in [17,18] represents not only the carboxyl group, but a number of bands in the range 1400 – 1290 cm^{-1} , which are attributed to the presence of type I collagen in biological tissue. As shown in Fig. 9 we confirm the “red shift” of this band for the synthesized composites af-

ter immersion in 1.5SBF for 3 days. The band centred at 1335 (1336) cm^{-1} can be described as a wagging vibration through the covalent bond formation with Ca^{2+} of partial dissolution silicocarnotite. The amount of observed “red shift” is determined by the conditions of the in vitro test, pH, temperature and concentration of the reagents in 1.5SBF solution. The bands at 1641 (1646) cm^{-1} and 1550 (1556) cm^{-1} can be assigned to the amide I and amide II from collagen [17,18,54].

Figure 10 concisely presents the evaluation of ionic concentration of Ca, P and Si in the liquid after in vitro test of the synthesized C-S composites after 3 days of soaking in 1.5SBF by ICP-AES analysis. From the data of Fig. 10, we can see that the Ca concentration for the two samples slightly increased from 89 mg/l (which is the concentration of Ca in 1.5SBF before soaking), to 179 mg/l (sample 1) and 164 mg/l (sample 2). Meanwhile, the concentration of P also increased from 1 mg/l in 1.5SBF before the test, to 22 mg/l (sample 1) and 4 mg/l (sample 2). From the depicted results we can conclude that (i) ion exchange of Ca and P increases their concentration in 1.5SBF and (ii) the formation of HA phase on the surface of the immersed samples, which would consume Ca and P, leads to a decrease in Ca and P concentration in 1.5SBF solution. From sample 2, the concentration of P is lower than the one in sample 1, in accordance to the weight ratio of the C and S as the parts of the composite. The lower P concentration leads to a conclusion that P may play an active role in the transformation of the sample surface during in vitro test. For instance, Agathopou-

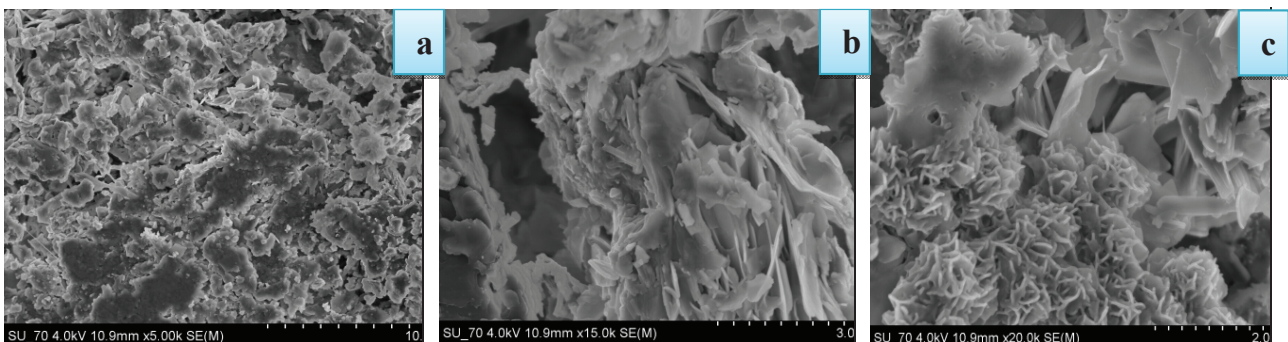


Figure 12. SEM for C-S sample (25:75 wt.%) at different magnifications: 5000× (a), 15000× (b) and 20000× (c)

los *et al.* [55] observed that in the case of CaO-MgO-SiO₂ glass, modified with B₂O₃, Na₂O, CaF₂ and P₂O₅ after very long immersion in SBF phosphorus concentration was rapidly decreased. Because the quantity of S for samples 1 and 2 is 75 and 25 wt.%, respectively, we can conclude from Fig. 10 that the concentration of Si for the sample 2 is higher than the one in sample 1. In accordance with X-ray diffraction data (Fig. 1) we could conclude that these changes (caused by dissolution and precipitation process, respectively) are more pronounced for carbonate hydroxyapatite (Ca₁₀(PO₄)₅CO₃(OH)F) and the C-S-P-H phase. This conclusion is in good agreement with literature data [56]. From the obtained ICP-AES results, we can conclude that after in vitro test of the prepared composites silicon containing carbonate substituted hydroxyapatite (Si-CO₃HA), may be formed on the surface of the immersed samples. This conclusion will be the subject of some future article.

Figures 11 and 12 show SEM images of the samples after in vitro test in 1.5SBF for 3 days in static conditions. The morphology of the samples after in vitro test in 1.5SBF for 3 days shows a relatively dense microstructure. This result indicated that the composites with ChS were endowed with excellent bioactivity. A similar morphology has been observed by other authors [57]. Figure 11b shows detailed microstructure of the fibre-side. From Fig. 11a,b it is noted that the nucleation of hydroxyapatite crystals were initiated from the surface of the collagen fibres and silicocarnotite, leading to the conjecture that there are some types of interactions between the HA crystals and collagen fibres. The presented SEM image at a high magnification value (Fig. 11c) clearly shows the presence of the concentrated spherical particles. They have a bright colour and have some pores denoting the formation and nucleation of an apatite layer. The presented SEM images also show that hydroxyapatite particles are connected to each other in the sample. For the C-S sample with 25:75 wt.% of the components, SEM image (Fig. 12c) shows a mixture of plate-like and needle-like HA crystals.

IV. Conclusions

The purpose of this work was to prepare, characterize and evaluate in vitro bioactivity of composites between collagen and silicocarnotite in the presence of chondroitin sulphate. Collagen type I, diluted in acetic acid, was mixed with silicocarnotite powder in a 25:75 and 75:25 weight ratio, in the presence of chondroitin sulphate. XRD of the prepared composites depicts the presence of carbonate containing hydroxyapatite and CaO-P₂O₅-SiO₂-H₂O crystalline phases, from the partially dissolved silicocarnotite glass-ceramics. FTIR observed that the chemical interaction between Ca²⁺ and COO⁻ and/or SO₃⁻ from the chondroitin sul-

phate and β-sheets structures might occur. In the sample with 75:25 wt.% collagen:silicocarnotite FTIR observed the “red shift” of C=O amide I, which related to the chemical interaction between Ca²⁺ and C=O: amide I. On the other hand, the B-type of carbonate containing hydroxyapatite in which CO₃²⁻→PO₄³⁻ is formed in situ into the composites. SEM of the composite with 75:25 wt.% collagen:silicocarnotite depicts the presence of nanosized hydroxyapatite whiskers. This observation confirmed the XRD and FTIR results.

After in vitro test in 1.5 SBF, XRD observed well defined hydroxyapatite peaks. Based on these results we can assume that the prepared composites are in vitro bioactive. FTIR depicted that the band centred at ~1335 cm⁻¹ could be ascribed to the covalent bond between Ca²⁺, from the partially dissolved phases and deprotonated carboxylate groups from the collagen. SEM proved that the sample prepared with chondroitin sulphate composites endowed excellent in vitro bioactivity. ICP-AES data lead to a conclusion that silicon containing carbonate substituted hydroxyapatite may be formed on the samples immersed in 1.5SBF solution.

Acknowledgements: The authors kindly acknowledge Dr. Tsvetelina Gerganova from AQUACHIM JSC-Bulgaria for her support for fitting of the FTIR spectra.

References

1. A. Sionkowska, J. Kozłowska, “Characterization of collagen/hydroxyapatite composite sponges as a potential bone substitute”, *Int. J. Biol. Macromol.*, **47** [4] (2010) 483–487.
2. J. Li, H. Sun, D. Sun, Y. Yao, F. Yao, K. Yao, “Biomimetic multicomponent polysaccharide/nano-hydroxyapatite composites for bone tissue engineering”, *Carbohydr. Polym.*, **85** [4] (2011) 885–894.
3. L. Zhang, P. Tang, M. Xu, W. Zhang, W. Chai, Y. Wang, “Effects of crystalline phase on the biological properties of collagen–hydroxyapatite composites”, *Acta Biomaterialia*, **6** [6] (2010) 2189–2199.
4. W. Schneiders, A. Reinstorf, M. Ruhnov, S. Rehberg, J. Heineck, I. Hinterseher, A. Biewener, H. Zwipp, S. Rammelt, “Effect of chondroitin sulfate on material properties and bone remodelling around hydroxyapatite/collagen composites”, *J. Biomed. Mater. Res.*, **85A** (2008) 638–645.
5. S.M. Partridge, “The chemistry of connective tissues. 1. The state of combination of chondroitin sulfate in cartilage”, *Biochem. J.*, **43** [3] (1948) 387–397.
6. W. Garnjanagoonchorn, L. Wongekalak, A. Engkagul, “Determination of chondroitin sulfate from different sources of cartilage”, *Chem. Eng. Process.*, **46** (2007) 465–471.
7. S.-H. Rhree, J. Tanaka, “Synthesis of hydroxyapatite/collagen/chondroitin sulfate nanocomposite by a novel precipitation method”, *J. Am. Ceram. Soc.*, **84** [2] (2001) 459–461.

8. S.-H. Rhee, J. Tanaka, "Effect of chondroitin sulfate on the crystal growth of hydroxyapatite", *J. Am. Ceram. Soc.*, **83** [8] (2000) 2100–2102.
9. S.-H. Rhee, J. Tanaka, "Self-assembly phenomenon of hydroxyapatite nanocrystals on chondroitin sulfate", *J. Mater. Sci.: Mater. Med.*, **13** (2002) 597–600.
10. S.-H. Rhee, Y. Suetsugu, J. Tanaka, "Biomimetic configurational arrays of hydroxyapatite nanocrystals on bio-organics", *Biomaterials*, **22** (2001) 2843–2847.
11. X. Xiao, D. He, F. Liu, R. Liu, "Preparation and characterization of hydroxyapatite/chondroitin sulfate composites by biomimetic synthesis", *Mater. Chem. Phys.*, **112** (2008) 838–843.
12. D. He, X. Xiao, F. Liu, R. Liu, "Chondroitin sulfate template-mediated biomimetic synthesis of nanoflake hydroxyapatite", *Appl. Surface Sci.*, **255** (2008) 361–364.
13. Y.S. Pek, Sh. Gao, M. Mohamed Arshad, K.-J. Lee, J. Ying, "Porous collagen-apatite nanocomposite foams as bone regeneration scaffolds", *Biomaterials*, **29** (2008) 4300–4305.
14. H. Jiang, X.-Y. Liu, G. Zhang, Y. Li, "Kinetics and template nucleation of self-assembled hydroxyapatite nanocrystallites by chondroitin sulfate", *J. Biol. Chem.*, **280** [51] (2005) 42061–42066.
15. G. Gafni, D. Septier, M. Goldberg, "Effect of chondroitin sulfate and biglycan on crystallization of hydroxyapatite under physiological conditions", *J. Crystal Growth*, **205** (1999) 618–623.
16. L. Radev, V. Hristov, I. Michailova, B. Samuneva, "Sol-gel bioactive glass-ceramics. Part I: Calcium phosphate silicate/wollastonite glass-ceramics", *Cent. Eur. J. Chem.*, **7** [3] (2009) 317–321.
17. L. Radev, V. Hristov, B. Samuneva, D. Ivanova, "Organic/Inorganic bioactive materials Part II: in vitro bioactivity of Collagen-Calcium Phosphate Silicate/Wollastonite hybrids", *Cent. Eur. J. Chem.*, **7** [4] (2009) 711–720.
18. L. Radev, M.H.V. Fernandes, I.M. Salvado, D. Kovacheva, "Organic/Inorganic bioactive materials Part III: in vitro bioactivity of gelatin/silicocarnotite hybrids", *Cent. Eur. J. Chem.*, **7** [4] (2009) 721–730.
19. G. Falini, S. Fermani, B. Palazzo, N. Roveri, "Helical domain collagen substrates mineralization in simulated body fluid", *J. Biomed. Mater. Res.*, **A87** [2] (2008) 470–476.
20. H.-W. Lee, J.-H. Kim, "Properties of hydration and strength of the sol-gel derived fine particle in the system CaO-P₂O₅-SiO₂", *J. Korean Ceram. Soc.*, **31** [10] (1994) 1231–1239.
21. Z. Gou, J. Chang, W. Zhai, "Preparation and characterization of novel bioactive dicalcium silicate ceramics", *J. Eur. Ceram. Soc.*, **25** (2005) 1507–1514.
22. Sh. Zou, J. Huang, S. Best, W. Bonfield, "Crystal imperfection studies of pure and silicon substituted hydroxyapatite using Raman and XRD", *J. Mater. Sci.: Mater. Med.*, **16** (2005) 1143–1148.
23. E.S. Thian, J. Huang, M. Vickers, S. Best, Z. Barber, W. Bonfield, "Silicon-substituted hydroxyapatite (SiHA): A novel calcium phosphate coating for biomedical applications", *J. Mater. Sci.*, **41** (2006) 709–714.
24. V. Jokanović, D. Izvonar, M.D. Dramićanin, B. Jokanović, V. Živojinović, D. Marković, B. Dačić, "Hydrothermal synthesis and nanostructure of carbonated calcium hydroxyapatite", *J. Mater. Sci.: Mater. Med.*, **17** (2006) 539–546.
25. I. Gibson, S. Best, W. Bonfield, "Chemical characterization of silicon-substituted hydroxyapatite", *J. Biomed. Mater. Res.*, **44** (1999) 422–428.
26. J. Anderson, S. Avera, B. Spliethoff, M. Linden, "Sol-gel synthesis of a multifunctional, hierarchically porous silica/apatite composite", *Biomaterials*, **26** (2005) 6827–6835.
27. N. Patel, S. Best, W. Bonfield, I. Gibson, K. Hing, E. Damien, P. Revell, "A comparative study on the in vitro behaviour of hydroxyapatite and silicon substituted hydroxyapatite granules", *J. Mater. Sci.: Mater. Med.*, **13** (2002) 1199–1208.
28. S.R. Federman, V.C. Costa, D.C. Vasconcelos, W.L. Vasconcelos, "Sol-gel SiO₂-CaO-P₂O₅ biofilm with surface engineered for medical application", *Mater. Res.*, **10** (2007) 177–181.
29. M. Cerruti, D. Greenspan, K. Powers, "Effect of pH ionic strength on the reactivity of Bioglass 45S", *Biomaterials*, **26** (2005) 1665–1674.
30. K. Salma, L. Berzina-Cimdina, N. Borodajenko, "Calcium phosphate bioceramics prepared from wet chemically precipitated powders", *Process. Applic. Ceram.*, **4** [1] (2010) 45–51.
31. I. Rehman, W. Bonfield, "Characterization of hydroxyapatite and carbonated apatite by photo acoustic FTIR spectroscopy", *J. Mater. Sci.: Mater. Med.*, **8** [1], (1997) 1–4.
32. E. Landi, G. Celotti, G. Logroscino, A. Tampieri, "Carbonated hydroxyapatite as bone substitute", *J. Eur. Ceram. Soc.*, **23** (2003) 2931–2937.
33. Y. Tanaka, S. Takata, K. Shimoe, M. Nakamura, A. Nagai, T. Toyama, K. Yamashita, "Conduction properties of non-stoichiometric hydroxyapatite whiskers for biomedical use", *J. Ceram. Soc. Jpn.*, **116** [7] (2008) 815–821.
34. M. Tamai, M. Nakamura, T. Issiki, K. Nishio, H. Endoh, A. Nakahira, "A metastable phase in thermal decomposition of Ca-deficient hydroxyapatite", *J. Mater. Sci.: Mater. Med.*, **14** (2003) 617–622.
35. S. Jalota, S. Bhaduri, A. C. Tas, "In vitro testing of calcium phosphate (HA, TCP, and biphasic HA-TCP) whiskers", *J. Biomed. Mater. Res.*, **A78**, (2006) 481–490.
36. K.J. Payne, A. Veis, "Fourier transform IR spectroscopy of collagen and gelatin solutions: Deconvolution of the amide I band for conformational studies", *Biopolymers*, **27** [11] (1988) 1749–1760.

37. D. Alili, "Polypeptide-based nanocomposite materials, *Ph.D. Thesis, Linköping University, Institute of Technology, Sweden*, 2008.
38. D. Liard, M. Mulvihill, J. Lillig, "Membrane-induced peptide structural changes monitored by infrared and circular dichroism spectroscopy", *Biophys. J.*, **145** (2008) 72–78.
39. C. Petibois, G. Gouspillou, K. Wehbe, J.-P. Delage, G. Délérís, "Analysis of type I and IV collagens by FT-IR spectroscopy and imaging for a molecular investigation of skeletal muscle connective tissue", *Anal. Bioanal. Chem.*, **400** (2011) 1961–1966.
40. S. Krimm, J. Bandekar, "Vibrational spectroscopy and conformation of peptides", *Adv. Protein Chem.*, **38** (1986) 181–364.
41. K. Belbachir, R. Noreen, G. Gouspillou, C. Petibois, "Collagen types analysis and differentiation by FTIR spectroscopy", *Anal. Bioanal. Chem.*, **395** [3] (2011) 829–837.
42. R. Mendelsohn, G. Mao, C. Flash, "Infrared reflection-absorption spectroscopy: principles and applications to lipid-protein interaction in Langmuir films", *Biochim. Biophys. Acta*, **1798** (2010) 788–800.
43. J. Quan, Y. Kang, W. Zhang, Z. Li, "Fabrication, chemical composition change and phase evolution of biomorphic hydroxyapatite", *J. Mater. Sci.: Mater. Med.*, **19** (2008) 3373–3383.
44. A. Stepuk, A. Veresov, V. Putlyayev, Y. Tretyakov, "The influence of NO_3^- , CH_3COO^- and Cl^- ions in calcium hydroxyapatite crystals", *Dokl. Phys. Chem.*, **412** (2007) 11–14.
45. Z.H. Cheng, A. Yasukawa, K. Kandori, T. Ishikawa, "FTIR study of incorporation of CO_2 into calcium hydroxyapatite", *J. Chem. Soc., Faraday Trans.*, **94** [10] (1998) 1501–1505.
46. M. Feet, X. Liu, P. King, "Accommodation of the carbonate ion in apatite: An FTIR and X-ray structure study of crystals synthesized at 2–4 GPa", *Am. Mineral.*, **89** (2004) 1422–1432.
47. M. Fleet, "Infrared spectra of carbonate apatites: ν_2 -Region bands", *Biomaterials*, **30** [8] (2009) 1473–1481.
48. G. Xu, I.A. Aksay, J.T. Groves, "Continuous crystalline carbonate apatite thin films. A biomimetic approach", *J. Am. Chem. Soc.*, **123** (2001) 2196–2203.
49. Th. Leventouri, A. Antonakos, A. Kyriacou, R. Venturelli, E. Liarokapis, V. Perdikatsis, "Crystal structure studies of human dental apatite as a function of age", *Int. J. Biomater.*, **2009** (2009) 1–6.
50. Z. Tomić, P. Makreski, B. Gajić, "Identification and spectra–structure determination of soil minerals: Raman study supported by IR spectroscopy and X-ray powder diffraction", *J. Raman Spectroscopy*, **41** [5] (2010) 582–586.
51. R. Ravisankar, G. Senthilkumar, S. Kiruba, A. Chandrasekaran, P. Jebakumar, "Mineral analysis of coastal sediment samples of Tuna, Gujarat, India", *Indian J. Sci. Technol.*, **3** [7] (2010) 774–780.
52. H. El Feki, Ch. Rey, M. Vignoles, "Carbonate ions in apatites: Infrared investigations in the $\nu_4 \text{CO}_3$ domain", *Calcified Tissue Int.*, **49** [4] (1991) 269–274.
53. A. Antonakos, E. Liarokapis, Th. Leventouri, "Micro-Raman and FTIR studies of synthetic and natural apatites", *Biomaterials*, **28** [19] (2007) 3043–3054.
54. E. Sachlos, D. Wahl, J. Triffitt, J. Czernuszka, "The impact of critical point drying with liquid carbon dioxide on collagen–hydroxyapatite composite scaffolds", *Acta Biomaterialia*, **4** [5] (2008) 1322–1331.
55. S. Agathopoulos, D.U. Tulyaganov, J.M.G. Ventura, S. Kannan, M.A. Karakassides, J.M.F. Ferreira, "Formation of hydroxyapatite onto glasses of the CaO-MgO-SiO_2 system with B_2O_3 , Na_2O , CaF_2 and P_2O_5 additives", *Biomaterials*, **27** [9] (2006) 1832–1840.
56. A. Slosarczyk, Z. Paszkiewicz, A. Zima, "The effect of phosphate source on the sintering of carbonate substituted hydroxyapatite", *Ceram. Int.*, **36** (2010) 577–582.
57. X. Liu, L. A. Smith, J. Hu, P. X. Ma, "Biomimetic nanofibrous gelatin/apatite composite scaffolds for bone tissue engineering", *Biomaterials*, **30** [12] (2009) 2252–2258.